

MODELING THE SHAPE OF WHEAT KERNELS WITH THE USE OF SOLIDS OF REVOLUTION

Andrzej Anders^{a*}

^a Department of Heavy-Duty Machines and Research Methodology, University of Warmia and Mazury in Olsztyn, ul. M. Oczapowskiego 11, 10-736 Olsztyn, Poland;
e-mail: anders@uwm.edu.pl, ORCID 0000-0001-6950-4141

* Corresponding author: e-mail: anders@uwm.edu.pl

ARTICLE INFO

Article history:
Received: April 2023
Received in the revised form: July 2023
Accepted: August 2023

Keywords:
3D scanner,
geometric model,
wheat kernels,
solid of revolution

ABSTRACT

Numerical models approximating a kernel shape in wheat cv. Eta were developed with the use of a 3D scanner and applied to analyze selected geometric properties of wheat kernels. Geometric models were built in ScanStudio HD PRO, FreeCAD, and MeshLab programs. Ten geometric models describing the shape of wheat kernels were generated with the use of basic geometric figures and drawing tools in FreeCAD. The geometry of numerical models and geometric models was compared in GOM Inspect. The surface area, volume, and accurate geometric dimensions of the developed models were determined. Deviations in the dimensions of geometric models were mapped. The relative error of surface area measurements was the lowest in solid of revolution obtained by rotating a polygonal chain around an axis at 0.36%. The relative error of measurement reached 4.44% in sphere and around 5% in solid of revolution obtained by rotating two curves around an axis and solid of revolution obtained by rotating three curves around an axis. The relative error of volume measurements was the lowest in rotational ellipsoid (spheroid) and ellipsoid at 3.58% and 4.48%, respectively. The developed geometric models can be used in research and design.

Introduction

Geometric models of raw materials facilitate the design of technical operations. These models are applied in the design of processing machines and devices. 3D models can be used for this purpose (Ayr et al., 2015; Becerra et al., 2022). 3D models describing the physical properties of the examined objects are applied to model processing operations with high accuracy (Datta and Halder, 2008; Pasha et al., 2016; Binelo et al., 2019). In most cases, numerical models are generated on the assumption that agri-food products are homogeneous and isotropic, and that they can be modeled with the use of regular shapes and figures (such as a cylinder, sphere, or a cone) (Gastón et al., 2002; Sinnott et al., 2021; Wiącek et al., 2021). Modern computers with a high computational power, and advanced software solutions for computer-aided design (CAD) and computational fluid dynamics (CFD) modeling support the development of complex geometric models (Favier et al., 1999; Verboven et al., 2004; Xiaolong et al., 2016). Models that accurately describe the shape of the analyzed objects,

including their individual traits, and which can be used in computer simulations, pose a challenge in research and design of processing machines in the agri-food sector (Entem et al., 2015; Zeren et al., 2018; Jian et al., 2020). The development of numerical models for designing machines and equipment is a time-consuming process (Goni et al., 2007; Yatskul et al., 2017).

Various geometric models have been described in the literature. A machine vision system was used by Jancsok et al. (2001) to build numerical models of pears cv. Konferencja. Sabliov et al. (2002) relied on image analysis techniques to model the volume and surface area of axially symmetric agri-food products. A thermal system for disinfecting fruit was developed based on 3D strawberry models generated with the use of a machine vision system (Scheerlinck et al., 2004). Kim et al. (2007) relied on computed tomography to build geometric models of food products with a complex shape. Goni et al. (2008) proposed a methodology for developing geometric models based on magnetic resonance imaging (MRI) scans. Mieszkal-ski (2013) developed computer models depicting the shape of carrots. Balcerzak et al. (2015) modeled the geometric properties of corn and oat kernels in the 3ds Max environment. Jiangang et al. (2021) described quantitative potato tuber phenotyping by 3D imaging. Models that accurately depict the shape of the examined objects can be generated with a 3D scanner and used to analyze the shape of entire objects or their parts (Rahmi and Ferruh, 2009; Anders et al., 2015). Zubko et al. (2022) developed a novel geometric model of wheat kernels with a displaced center of mass and conducted theoretical and experimental analyses of kernel orientation. Kernel orientation was determined during multiple interactions between wheat kernels and an inclined plane. The proposed model of a wheat kernel had a displaced center of mass, and it was composed of differently shaped hemispheres at each end and a truncated cone. Dongxu et al. (2020) analyzed the shape and dimensions of the seeds of 12 soybean varieties. The shape of soybean seeds approximated an ellipsoid, and their sphericity ranged from 80.57% to 95.42%. The cited authors used the multi-sphere method to generate 5-, 9-, and 13-sphere models of individual seeds and groups of seeds belonging to three soybean varieties. They found that 5-, 9-, and 13-sphere models developed with the multi-sphere method were suitable for modeling the seeds of different soybean varieties, and the simulated result of the multi-sphere model was superior to the result of the ellipsoid model developed based on the ellipsoid equation. Soybeans characterized by high sphericity can be modeled with a 5-sphere model, whereas seeds with low sphericity can be represented by 9- or 13-sphere models.

Long et al. (2020) analyzed the shape of maize seeds and concluded that the developed model can be simplified to five shapes, i.e., a horse tooth, a truncated triangular pyramid, an ellipsoid cone, a spheroid, and an irregular shape. The cited authors reported a certain functional relationship between the characteristic dimensions of each shape model. Based on this observation, the multi-sphere method was applied to generate four shape models of maize seeds with different accuracy. Long et al. (2021) analyzed the multi-sphere model which is widely applied to depict the shape of maize seeds in discrete element modeling. Shuai et al., (2022) relied on the discrete element method (DEM) to propose a method for modeling non-spherical particles. The cited study involved edible sunflower seeds, and models of individual seeds and groups of seeds were generated by analyzing the triaxial dimensions and three-dimensional volumes of sunflower seeds and simplifying seed shapes. Tianyue et al. (2018) used the DEM approach to develop a model of soybean seeds based on measurements of seed

shape and size. They found that the shape of soybean seeds can be approximated by an ellipsoid and that differences in seed size follow normal distribution. A functional relationship between primary and secondary dimensions was also reported. An approach for modeling soybean seeds was proposed based on the multi-sphere (MS) method. A soybean seed was simplified to an ellipsoid with an average size of one hundred randomly selected seeds. A model of a single soybean was generated by filling the spheres within the ellipsoid. To model a group of soybean seeds, the primary dimension was generated according to normal distribution, and the remaining secondary dimensions were calculated based on their relationships with the primary dimension. This approach was used to model a group of seeds with different sizes and distributions. The experiment involved the seeds of four soybean varieties.

However, the accuracy with which the geometric parameters of the examined objects were represented by the proposed models was not analyzed in the cited studies. Therefore, the aim of this study was to build geometric models of wheat kernels based on geometric figures and solids of revolution. The resulting geometric models were compared with the models generated by 3D scanning. The surface area, volume, and dimensions of wheat kernels and the developed models were compared. The paper attempts to check what differences exist for the geometrical parameters of the proposed solids of revolution in comparison to the shape of the seed kernel.

Materials and methods

The experimental material comprised kernels of wheat cv. Eta (*Triticum aestivum* L.) purchased from Małopolska Hodowla Roślin Sp. z o.o. in Kobierzyce, Poland (50.96638°N, 16.92001°E). Thirty kernels without visible signs of damage were selected randomly for the study. The analyzed kernels were spindle shaped. Before 3D scanning, they were stored in a refrigerator at a constant temperature of $6\pm 1^\circ\text{C}$ and 60% humidity. The length, width, and thickness of wheat kernels were measured with a digital caliper within the accuracy of $d=0.01$ mm (Fig. 1). Kernels were weighed on the Radwag WAA 100/C/2 digital scale to the nearest 0.0001 g. Data were processed statistically in Statistica 10 at the significance level of $\alpha = 0.05$. Kernels were scanned with the NextEngine 3D scanner with a resolution of 248 pixels per mm^2 and pixel size of 0.13 mm. Numerical 3D models of wheat kernels were developed in ScanStudio HD PRO (<http://www.nextengine.com>). The surface area and volume of wheat kernels were determined based on 3D models in MeshLab (<http://meshlab.sourceforge.net/>).

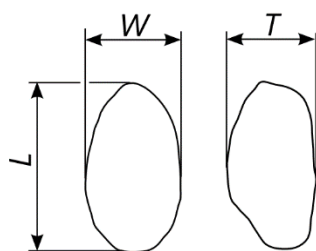


Figure 1. Basic dimensions of wheat kernels: L – length (mm), W – width (mm), T – thickness (mm)

The surface area and volume of the geometric models presented in Figure 2 were calculated. These parameters were calculated based on the results of caliper measurements with the use of mathematical formulas. The surface area and volume of models based on solids of revolution were calculated in FreeCAD (<https://www.freecadweb.org>).

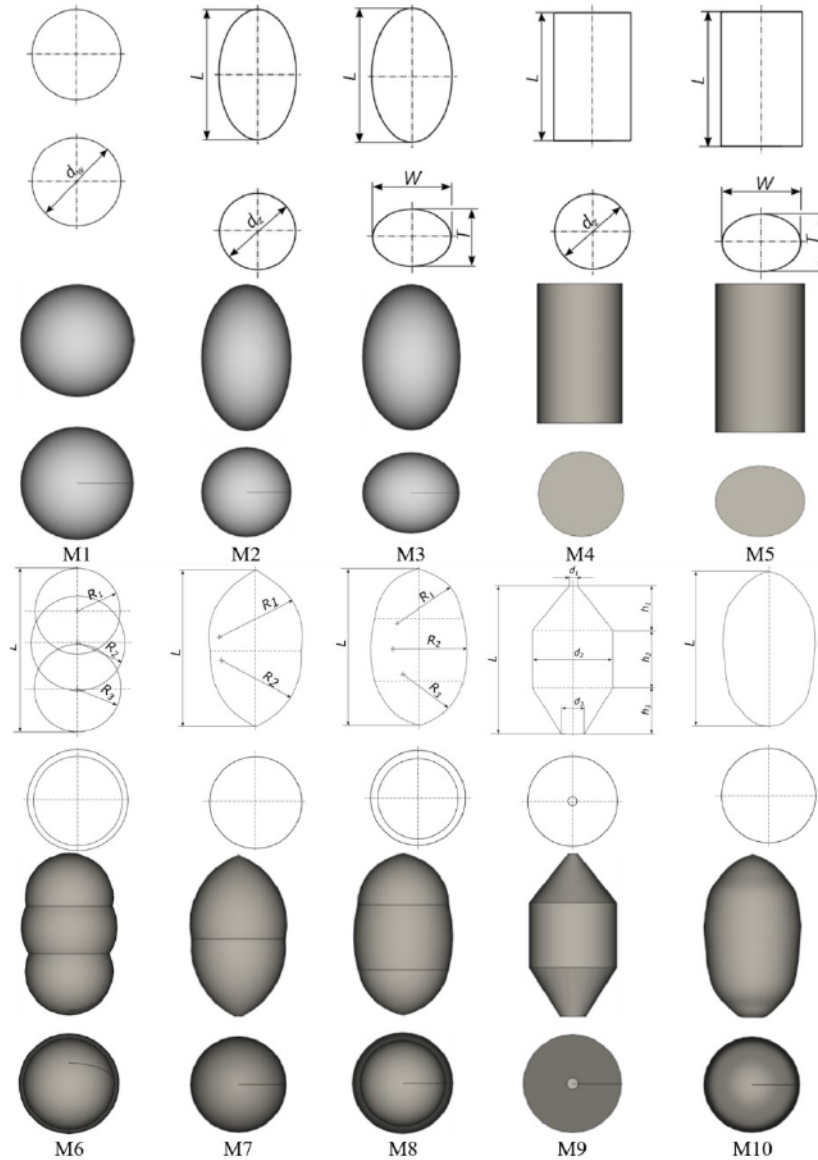


Figure 2. Geometric models of wheat kernels. L – length (mm), W – width (mm), T – thickness (mm), $R1$ – radius (mm), $R2$ – radius (mm), $R3$ – radius (mm)

The following mathematical formulas were used to estimate the volume and surface area of wheat kernels:

- sphere (M1):

$$A_{M1} = \pi \cdot d_w^2 \quad (1)$$

$$V_{M1} = \frac{\pi \cdot d_w^3}{6} \quad (2)$$

- rotational ellipsoid (spheroid) (M2), if: $\frac{L}{2} > \frac{d_z}{2}$

then:

$$A_{M2} = \frac{4 \cdot \pi \cdot d_z^2 + \pi \cdot L \cdot d_z \cdot e \cdot \arcsin(e)}{8} \quad (3)$$

where:

$$e = \sqrt{1 - \frac{d_z^2}{L^2}} \quad (4)$$

$$V_{M2} = \frac{\pi \cdot d_z^2 \cdot L}{6} \quad (5)$$

- ellipsoid (M3):

$$A_{M3} = 2 \cdot \pi \cdot \left(\left(\frac{L}{2} \right)^2 + \frac{\frac{T}{2} \cdot \left(\frac{L}{2} \right)^2}{\sqrt{\left(\frac{W}{2} \right)^2 - \left(\frac{L}{2} \right)^2}} \cdot F(\Theta, m) + \frac{T}{2} \cdot \sqrt{\left(\frac{W}{2} \right)^2 - \left(\frac{L}{2} \right)^2} \cdot E(\Theta, m) \right) \quad (6)$$

where:

$$m = \frac{L^2 \cdot T^2 - L^4}{T^2 \cdot W^2 - L^2 \cdot T^2} \quad (7)$$

$$\Theta = \arcsin \sqrt{\frac{\sqrt{W^2 - L^2}}{|W|}} \quad (8)$$

$F(\Theta, m)$ and $E(\Theta, m)$ are incomplete elliptic integrals of the first and second kind (Bronsztejn et al., 2009).

$$V_{M3} = \frac{\pi \cdot T \cdot W \cdot L}{6} \quad (9)$$

- cylinder (M4):

$$A_{M4} = \pi \cdot d_z \cdot L + 2 \cdot \pi \cdot \left(\frac{d_z}{2}\right)^2 \quad (10)$$

$$V_{M4} = \frac{\pi \cdot d_z^2 \cdot L}{4} \quad (11)$$

- elliptic cylinder (M5):

$$A_{M5} \approx \pi \cdot L \cdot \left(\frac{3}{4} \cdot (W + T) - \sqrt{\frac{W \cdot T}{4}} \right) + 2 \cdot \pi \cdot \frac{W \cdot T}{4} \quad (12)$$

$$V_{M5} = \frac{\pi \cdot T \cdot W \cdot L}{4} \quad (13)$$

In models M1, M2, and M4, geometric mean diameters were determined with the below formulas:

$$d_w = \frac{L + W + T}{3} \quad (14)$$

$$d_z = \frac{W + T}{2} \quad (15)$$

Model M6 consisted of three spheres, and it was generated in FreeCAD based on images of wheat kernels (Fig. 3a). The images were acquired with the Plustek OpticPro ST24 flatbed scanner with a resolution of 120 dpi. The contour of a wheat kernel was drawn with an arc tool based on three points on the perimeter. Model M7 was solid of revolution obtained by rotating two curves around an axis, and it was generated based on images of wheat kernels (Fig. 3b). The contour of a wheat kernel was drawn with an arc tool based on three points on the perimeter. Two arcs with radii R_1 and R_2 were obtained. A similar procedure was applied to develop model M3, where the contour of a wheat kernel was drawn with the use of three arcs with radii R_1 , R_2 , and R_3 (Fig. 3c). Model M9 was a solid of revolution obtained by rotating a polygonal chain around an axis, and it was also generated based on images of wheat kernels (Fig. 3d).

Model M10 was a solid of revolution obtained by rotating a complex curve around an axis (B-spline curve passing through control points) (Fig. 3e). The surface area and volume of the generated geometric models were determined with the use of the FCInfo macro definition in FreeCAD. Geometric models were compared with 3D models in GOM Inspect (<http://www.gom.com>).

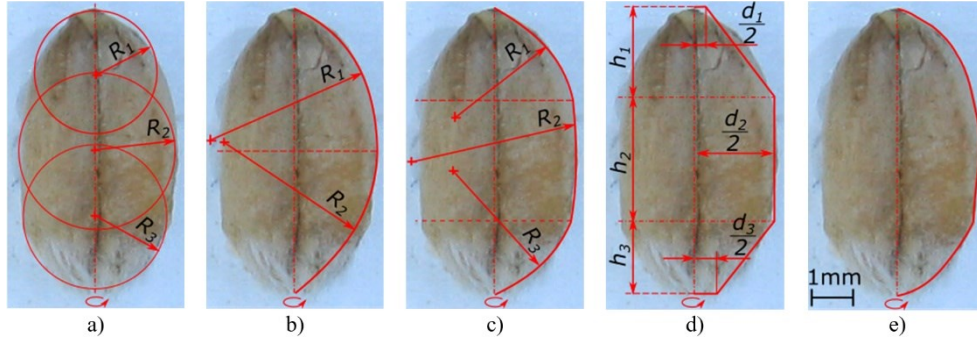


Figure 3. Contours for generating models of wheat kernels: a) M6; b) M7; c) M8; d) M9; e) M10.

The relative error for the surface area and volume was calculated according to the formulas:

$$\delta_A = \frac{|A - A_{MX}|}{A} \cdot 100\% \quad (16)$$

$$\delta_V = \frac{|V - V_{MX}|}{V} \cdot 100\% \quad (17)$$

where:

- A – wheat kernel surface area determined by 3D scanning, (mm²)
- A_{MX} – wheat kernel surface area of a geometric model, (mm²)
- V – wheat kernel volume determined by 3D scanning, (mm³)
- V_{MX} – wheat kernel volume of a geometric model, (mm³)

Results and discussion

Wheat cv. Eta produces round kernels that are easily removed from spikelets. Kernels have a crease on the ventral side, and floury or vitreous endosperms. Grain mass was determined at 0.0396 g in the smallest kernels and 0.0654 g in the largest kernels. Based on the results of 3D scans, the surface area of wheat kernels was determined in the range of 55.49 mm² to 79.54 mm², with an average of 64.73 mm². The kernel volume ranged from 30.43 mm³ to 54.32 mm³, with an average of 40.76 mm³ (Table 1).

The average dimensions, surface area, and volume of wheat kernels are presented in Table 1.

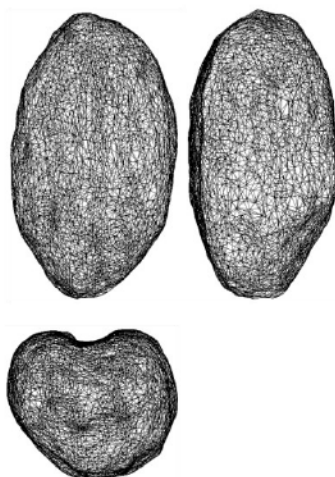


Figure 4. Numerical model of a wheat kernel composed of a triangle mesh.

Table 1.
Geometric properties of wheat kernels

Variable	Average	Coefficient of variation	Standard deviation
L (mm)	6.52	5.98	0.39
W (mm)	3.69	5.96	0.22
T (mm)	3.06	6.20	0.19
A^{3D} (mm ²)	64.73	8.20	5.31
V^{3D} (mm ³)	40.76	12.83	5.23
m (mg)	0.05	10.00	0.005

^{3D}- 3D scanning

Significant differences between the average surface area and volume of wheat kernels were determined with the Kruskal-Wallis non-parametric test. The significance of differences in the parameters of kernels determined based on 3D scanning, calculated using mathematical formulas, and calculated using geometric models is presented in Tables 2 and 3. The average surface area of wheat kernels determined based on the 3D numerical model did not differ significantly from the average surface area of sphere (M1) and solid of revolution obtained by rotating a polygonal chain around an axis (M9), but it differed significantly from the average surface area of the remaining geometric models.

Table 2.
Significance of differences in the average surface area of wheat kernels

Surface area A (Kruskal-Wallis test), $H(10, N=330)=205.6180$; $p=0.000$, Multiple comparison test				
Method of measurement	Valid N	Sum of ranks	Mean rank	Mean
3D	30	3968.00	132.26	64.73 ^b
M1	30	2906.50	96.88	61.71 ^{ab}

Modeling the shape...

Surface area A (Kruskal-Wallis test), $H(10, N=330)=205.6180$; $p=0.000$, Multiple comparison test				
Method of measurement	Valid N	Sum of ranks	Mean rank	Mean
M2	30	2034.50	67.81	59.54 ^a
M3	30	2206.50	73.55	60.04 ^a
M4	30	8903.50	296.78	87.27 ^e
M5	30	8887.00	296.23	87.27 ^e
M6	30	6549.00	218.30	73.44 ^d
M7	30	5027.50	167.58	68.04 ^c
M8	30	4947.00	164.90	67.92 ^c
M9	30	3873.00	129.10	64.41 ^b
M10	30	5312.50	177.08	69.09 ^c

Values with the same letters in columns do not differ significantly; a, b, c, d, e ($P \leq 0.05$). The average volume of wheat kernels determined based on the 3D numerical model did not differ significantly from the average volume of geometric models based on a rotational ellipsoid (M2) and an ellipsoid (M3).

Table 3.

Significance of differences in the average volume of wheat kernels

Volume V (Kruskal-Wallis test), $H(10, N=330)=172.4067$; $p=0.000$, Multiple comparison test				
Method of measurement	Valid N	Sum of ranks	Mean rank	Mean
3D	30	2722.00	90.73	40.76 ^{ab}
M1	30	4501.50	150.05	45.67 ^{cd}
M2	30	2129.50	70.98	39.12 ^a
M3	30	1976.00	65.86	38.75 ^a
M4	30	8180.50	272.68	58.68 ^f
M5	30	8045.50	268.18	58.12 ^f
M6	30	6509.50	216.98	52.33 ^e
M7	30	5609.50	186.98	49.44 ^e
M8	30	5401.50	180.05	48.98 ^{de}
M9	30	3779.00	125.96	43.80 ^{bc}
M10	30	5760.50	192.01	50.02 ^e

Values with the same letters in columns do not differ significantly; a, b, c, d, e, f ($p \leq 0.05$). The distribution of kernel surface area in 3D models and geometric models is presented in Figure 5a, and the distribution of kernel volume in 3D models and geometric models is presented in Figure 5b.

If we assume that kernel dimensions were measured accurately with the 3D scanner, the obtained data can be used as a reference to compare the results of caliper measurements and to approximate the shape of wheat kernels based on the developed geometric models. The relative error between 3D measurements and geometric models was referred to as a measurement error. As demonstrated in Figure 6a, the relative error of surface area measurements was the lowest (0.36%) in solid of revolution obtained by rotating a polygonal chain around an axis (M9). The relative error of measurement reached 4.44% in sphere (M1), and around 5% in solid of revolution obtained by rotating two curves around an axis (M7) and solid of revolution obtained by rotating three curves around an axis (M8). In the remaining models,

the relative error exceeded 6%. The relative error of volume measurements (Fig. 6b) was the lowest in spheroid (M2) (3.58%) and ellipsoid (M3) (4.48%), and it exceeded 7.74% in the remaining models.

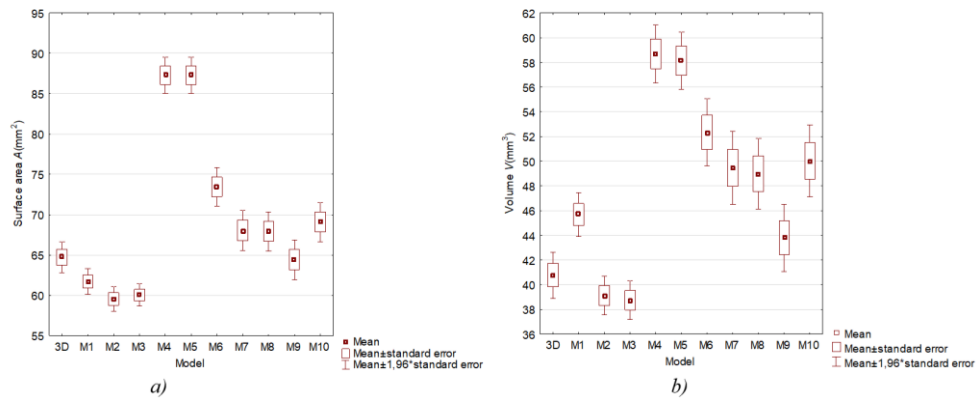


Figure 5. Parameters of normal distribution: a) surface area of wheat kernels, b) volume of wheat kernels

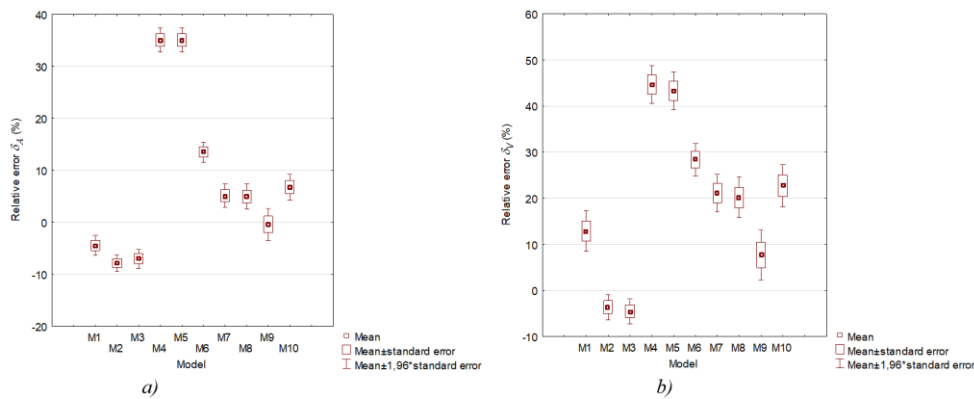


Figure 6. Relative error in the geometric parameters of wheat kernels measured with the use of geometric models and 3D scans: a) surface area, b) volume

Boryga and Kołodziej (2022) relied on a reverse engineering approach to model sugar beet roots using 3D design tools in the CAD environment. Root geometry was rendered based on a point cloud from 3D scans. The point cloud was used to build a triangle mesh covering triangle nodes. The cited authors did not measure deviations between the generated models and 3D scans. Caiyun et al. (2023) developed an ellipsoid modeling method to simulate the movement of wheat kernels with high accuracy. They described the structural parameters, motion equations, and contact judgement methods applied in modeling, and the structural

dimensions of wheat kernels. They found that the ellipsoid model was more accurate and robust than the multi-sphere model. The deviations in the generated models were not measured. In the present study, the deviations between kernel dimensions measured with the use of geometric models and 3D numerical models were determined in GOM Inspect (<https://www.gom.com>) (Fig. 7). Areas with the lowest deviations in the measured parameters are marked in green, and areas with the greatest deviations are marked in blue and red.

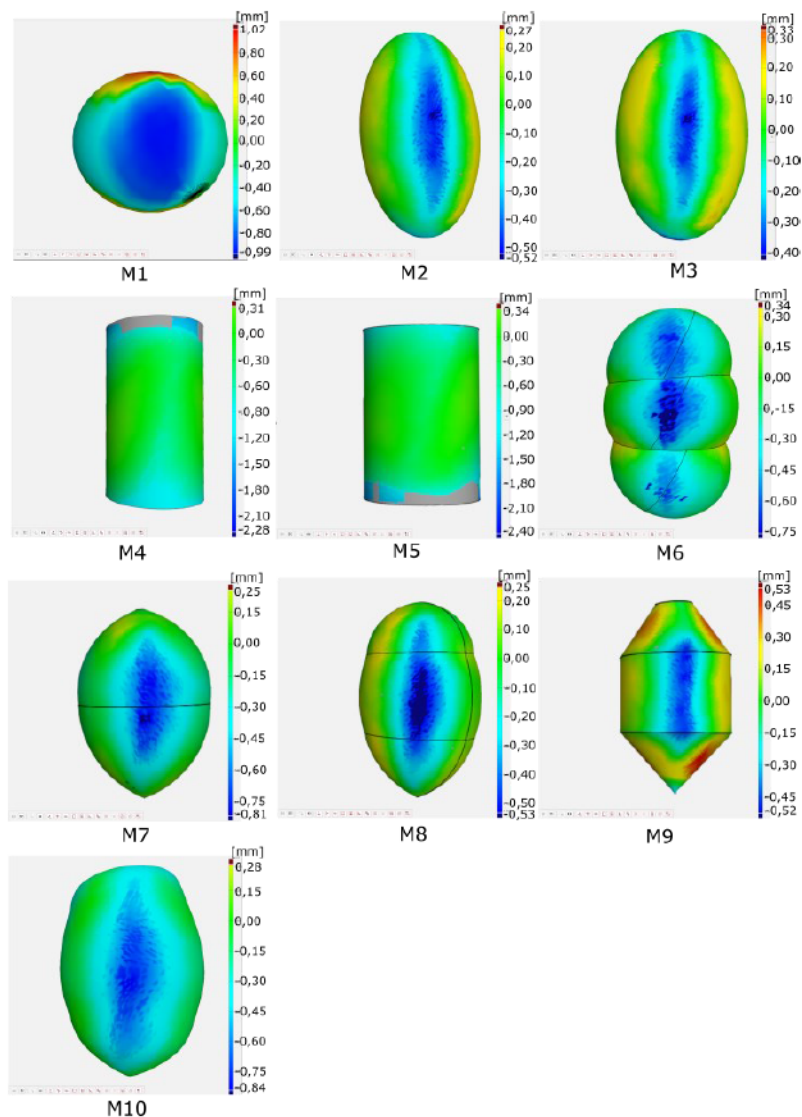


Figure 7. Maps of deviations in the dimensions of wheat kernels measured with the use of different models

The distribution of positive (+) and negative (-) deviations in kernel dimensions measured using geometric models and the 3D numerical model is presented in Figures 8a and 8b.

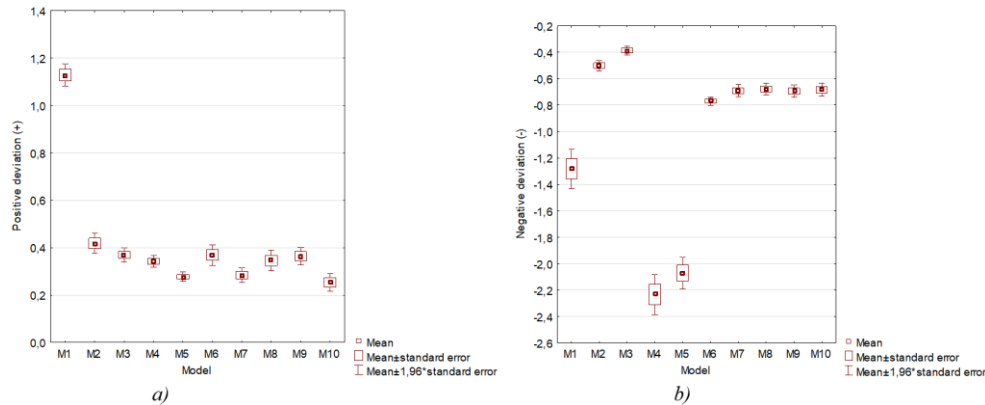


Figure 8. Parameters of normal distribution: a) positive deviation (+) in kernel dimensions, b) negative deviation (-) in kernel dimensions

The average positive deviation (+) in kernel parameters was the lowest in solid of revolution obtained by rotating a complex curve around an axis (M10) at 0.25 mm. The average positive deviation (+) in kernel parameters measured with sphere (M2), ellipsoid (M3), cylinder (M4), elliptic cylinder (M5), three spheres (M6), solid of revolution obtained by rotating two curves around an axis (M7), solid of revolution obtained by rotating three curves around an axis (M8) and solid of revolution obtained by rotating a polygonal chain around an axis (M9) ranged from 0.27 mm to 0.41 mm (Table 4).

Table 4.

Significance of differences in average positive deviation (+) in the geometric models of wheat kernels

Maximum deviation (+) (Kruskal-Wallis test), H (9, N=300)=130.8557; p=0.000, Multiple comparison test				
Method of measurement	Valid N	Sum of ranks	Mean rank	Mean
M1	30	8565.00	285.500	1.12 ^d
M2	30	5662.50	188.75	0.41 ^{ab}
M3	30	5004.00	166.80	0.36 ^b
M4	30	4394.00	146.46	0.34 ^a
M5	30	2623.50	87.45	0.27 ^c
M6	30	4703.50	156.78	0.36 ^{ab}
M7	30	3019.50	100.65	0.28 ^c
M8	30	4166.50	138.88	0.34 ^a
M9	30	4834.50	161.15	0.36 ^{ab}
M10	30	2177.00	72.56	0.25 ^c

Values with the same letters in columns do not differ significantly; a, b, c, d (P ≤ 0.05)

The average positive deviation (+) in kernel parameters was highest in the sphere (M1) at 1.12 mm. The average negative deviation (-) in kernel parameters determined with spheroid (M2), ellipsoid (M3), three spheres (M6), solid of revolution obtained by rotating two curves around an axis (M7), solid of revolution obtained by rotating three curves around an axis (M8), solid of revolution obtained by rotating a polygonal chain around an axis (M9) and solid of revolution obtained by rotating a complex curve around an axis (M10) ranged from -0.38 mm to -0.76 mm. The average negative deviation (-) in sphere (M1) reached 1.28 mm. The highest average negative deviation (-) was noted when kernel parameters were estimated with the use of cylinder (M4) (-2.23 mm) and elliptic cylinder (M5) (-2.07 mm) (Table 5).

Table 5.

Significance of differences in average negative deviation (-) in the geometric models of wheat kernels

Minimum deviation (-) (Kruskal-Wallis test), $H(9, N=300)=244.7976$; $p=0.000$, Multiple comparison test				
Method of measurement	Valid N	Sum of ranks	Mean rank	Mean
M1	30	2183.00	72.76	-1.28 ^e
M2	30	7370.00	245.66	-0.50 ^b
M3	30	8294.00	276.46	-0.38 ^b
M4	30	891.50	29.71	-2.23 ^c
M5	30	1087.50	36.25	-2.07 ^d
M6	30	4179.50	139.31	-0.76 ^a
M7	30	5232.50	174.41	-0.69 ^a
M8	30	5334.50	177.81	-0.67 ^a
M9	30	5221.00	174.03	-0.69 ^a
M10	30	5356.50	178.55	-0.68 ^a

Values with the same letters in columns do not differ significantly; a, b, c, d, e ($P \leq 0.05$)

Conclusions

Selected geometric parameters of wheat kernels were compared with the use of numerical models generated by 3D scanning, geometric models based on geometric figures, and geometric models developed with the use of drawing tools in CAD software. The surface area, volume, and dimensions of the modeled kernels were compared. The following conclusions can be formulated based on the presented results:

1. The surface area of wheat kernels was most accurately determined with the use of geometric models where the relative error of measurement did not exceed 5%. The above criterion was met by sphere (M1), solid of revolution obtained by rotating two curves around an axis (M7), solid of revolution obtained by rotating three curves around an axis (M8) and solid of revolution obtained by rotating a polygonal chain around an axis (M9). The relative error of surface area measurements was higher in spheroid (M2), ellipsoid (M3), cylinder (M4), elliptic cylinder (M5), three spheres (M6) and solid of revolution obtained by rotating a complex curve around an axis (M10) at 7.82%, 6.98%, 35.05%, 13.5%, and 6.08%, respectively.

2. The volume of wheat kernels was most accurately depicted by spheroid (M2) and ellipsoid (M3). In these models, the relative error of volume measurements did not exceed 4.48%. In the remaining models, the relative error of volume measurements was higher in the range of 7.75% to 44.62%.
3. The average positive deviation (+) was the lowest in solid of revolution obtained by rotating a complex curve around an axis (M10), where the modeled dimensions differed from real-world dimensions by only 0.25%. The lowest average negative deviation (-) was noted in ellipsoid (M3), where the modeled dimensions differed from real-world dimensions by 0.37%.
4. Numerical models generated with the use of a 3D scanner can be applied to determine the geometric parameters of whole kernels and their fragments. Numerical models are particularly useful for performing accurate measurements of the surface area, volume, and geometric dimensions, and comparing the results with other geometric models. These models can be applied in design and in digital simulations of processing operations. As an example, geometric models can be used in simulation studies of grain movement in air ducts, grain arrangement on working elements of cleaning and sorting machines, coating grain surface with chemicals, filling grain tanks, grain movement on working units of agricultural machines.

Bibliography

- Anders, A., Markowski, P., Kaliniewicz, Z. (2015). Numerical modelling of agricultural products on the example of bean and yellow lupine seeds. *International Agrophysics*, 29(4), 397-403.
- Ayr, U., Tamborrino, A., Catalano, P., Bianchi, B., Leone, A. (2015). 3D computational fluid dynamics simulation and experimental validation for prediction of heat transfer in a new malaxer machine. *Journal of Food Engineering*, 154, 30-38.
- Balcerzak, K., Weres, J., Górna, K., Idziaszek, P. (2015). Modeling of agri-food products on the basis of solid geometry with examples in Autodesk 3ds Max and finite element mesh generation. *Journal of Research and Applications in Agricultural Engineering*, 60(2), 5-8.
- Becerra, L. D., Zuluaga, M., Mayorga, E. Y., Moreno, F. L., Ruiz, R. Y., Escobar, S. (2022). Cocoa seed transformation under controlled process conditions: Modelling of the mass transfer of organic acids and reducing sugar formation analysis. *Food and Bioproducts Processing*, 136, 211-225.
- Binelo, M. O., de Lima, R. F., Khatchatourian, O. A., Stransky, J. (2019). Modelling of the drag force of agricultural seeds applied to the discrete element method. *Biosystems Engineering*, 178, 168-175.
- Boryga, M., Kołodziej, P. (2022). Reverse Engineering in Modeling Agricultural Products. *Agricultural Engineering*, 26(1), 105-117.
- Caiyun, L., Zhen, G., Hongwen, L., Jin, H., Qingjie, W., Xuyang, W., Xiuhong, W., Shan, J., Jing, X., Dong, H., Yunxiang, L. (2023). An ellipsoid modelling method for discrete element simulation of wheat seeds. *Biosystems Engineering* 226, 1-15.
- Datta, A.K., Halder, A. (2008). Status of food process modeling and where do we go from here (synthesis of the outcome from brainstorming). *Comprehensive Reviews in Food Science and Food Safety* 7, 117-120.
- Dongxu, Y., Jianqun, Y., Yang, W., Long, Z., Yajun, Y. (2020). A general modelling method for soybean seeds based on the discrete element method. *Powder Technology*, 372, 212-226.
- Entem, E., Barthe, L., Cani, M.P., Cordier, F., Van de Panne, M. (2015). Modeling 3D animals from a side-view sketch. *Computers & Graphics*, 46, 221-230.

- Favier, J.F., Abbaspour-Fard, M.H., Kremmer, M., Raji, A.O. (1999). Shape representation of axisymmetrical, non-spherical particles in discrete element simulation using multi-element model particles. *Engineering Computations*, 16, 467-480.
- FreeCAD 0.20.2. 2023. <https://www.freecadweb.org>.
- Gastón, A.L., Abalone, R.M., Giner, S.A. (2002). Wheat drying kinetics. Diffusivities for sphere and ellipsoid by finite elements. *Journal of Food Engineering*, 52(4), 313-322.
- GOM Inspect. 2023. <https://www.gom.com>.
- Goni, S.M., Purlis, E., Salvadori, V.O. (2007). Three-dimensional reconstruction of irregular food-stuffs. *Journal of Food Engineering* 82, 536-547.
- Goni, S.M., Purlis, E., Salvadori, V.O. (2008). Geometry modeling of food materials from magnetic resonance imaging. *Journal of Food Engineering*, 88, 561-567.
- Jancsok, P.T., Clijmans, L., Nicolai, B.M., De Baerdemaeker, J. (2001). Investigation of the effect of shape on the acoustic response of 'conference' pears by finite element modeling. *Postharvest Biology and Technology*, 23, 1-12.
- Jian, X., Xiaoming, W., Zhenbang, Z., Weibin, W. (2020). Discrete element modeling and simulation of soybean seed using multi-spheres and super-ellipsoids. *IEEE Access*, 8, 222672-222683.
- Jiangang, L., Xiangming, X., Yonghuai, L., Zexi, R., Melvyn, L. S., Liping, J., Bo, L. (2021). Quantitative potato tuber phenotyping by 3D imaging. *Biosystems Engineering*, 210, 48-59.
- Kim, J., Moreira, R.G., Huang, Y., Castell-Perez, M.E. (2007). 3-D dose distributions for optimum radiation treatment planning of complex foods. *Journal of Food Engineering*, 79, 312-321.
- Long, Z., Jianqun, Y., Liusuo, L., Yajun, Y., Dongxu, Y., Kai, S., Yang, W. (2021). Study on key issues in the modelling of maize seeds based on the multi-sphere method. *Powder Technology*, 394, 791-812.
- Long, Z., Jianqun, Y., Yang, W., Dongxu, Y., Yajun, Y. (2020). A study on the modelling method of maize-seed particles based on the discrete element method. *Powder Technology*, 374, 353-376.
- MeshLab Visual Computing Lab – ISTI – CNR. (2013). <http://meshlab.sourceforge.net>.
- Mieszkalowski, L. (2013). Computer-aiding of mathematical modeling of the carrot (*Daucus carota* L.) root shape. *Annals of Warsaw University of Life Sciences – SGGW. Agriculture*, 61, 17-23.
- NextEngine User Manual. (2010). <http://www.nextengine.com>.
- Pasha, M., Hare, C., Ghadiri, M., Gunadi, A., Piccione, P.M. (2016). Effect of particle shape on flow in discrete element method simulation of a rotary batch seed coater. *Powder Technology*, 296, 29-36.
- Rahmi, U., Ferruh, E. (2009). Potential use of 3-dimensional scanners for food process modeling. *Journal of Food Engineering*, 93, 337-343.
- Sabliov, C.M., Bolder, D., Keener, K.M., Farkas, B.E. (2002). Image processing method to determine surface area and volume of axi-symmetric agricultural products. *International Journal of Food Properties*, 5, 641-653.
- Scheerlinck, N., Marquenie, D., Jancsok, P.T., Verboven, P., Moles, C.G., Banga, J.R., Nicolai, B.M. (2004). A model-based approach to develop periodic thermal treatments for surface decontamination of strawberries. *Postharvest Biology and Technology*, 34, 39-52.
- Shuai, W., Zhihong, Y., Aorigele, W.Z. (2022). Study on the modeling method of sunflower seed particles based on the discrete element method. *Computers and Electronics in Agriculture*, 198, 1-16.
- Sinnott, M. D., Harrison, S. M., Cleary, P. W. (2021). A particle-based modelling approach to food processing operations. *Food and Bioprocess Processing*, 127, 14-57.
- Tianyue, X., Jianqun, Y., Yajun, Y., Yang, W. (2018). A modelling and verification approach for soybean seed particles using the discrete element method. *Advanced Powder Technology*, 29, 3274-3290.
- Verboven, P., De Baerdemaeker, J., Nicolai, B.M. (2004). Using computational fluid dynamics to optimize thermal processes. In: Richardson. P. (Ed.), *Improving the Thermal Processing of Foods*. CRC Press. Boca Raton, FL, 82-102.

- Wiącek, J., Gallego, E., Parafiniuk, P., Kobyłka, R., Banda, M., Horabik, J., Molenda, M. (2021). Experimental analysis of wheat-wall friction and grain flow in a steel silo with corrugated walls. *Biosystems Engineering*, 209, 216-231.
- Xiaolong, L., Yitao, L., Qingxi, L. (2016). Simulation of seed motion in seed feeding device with DEM-CFD coupling approach for rapeseed and wheat. *Computers and Electronics in Agriculture*, 131, 29-39.
- Yatskul, A., Lemiere, J. P., Cointault, F. (2017). Influence of the divider head functioning conditions and geometry on the seed's distribution accuracy of the air-seeder. *Biosystems Engineering*, 161, 120-134.
- Zeren, C., Jianqun, Y., Duomei, X., Yang, W., Qiang, Z., Luquan, R. (2018). An approach to and validation of maize-seed-assembly modelling based on the discrete element method. *Powder Technology*, 328, 167-183.
- Zubko, V., Sirenko, V., Kuzina, T., Onychko, V., Sokolik, S., Roubik, H., Koszel, M. & Shchur, T. (2022). Modelling Wheat Grain Flow During Sowing Based on the Model of Grain with Shifted Center of Gravity. *Agricultural Engineering*, 26(1), 25-37.

MODELOWANIE KSZTAŁTU ZIARNA PSZENICY ZA POMOCĄ BRYŁ OBROTOWYCH

Streszczenie. Celem pracy było zbudowanie za pomocą skanera 3D modeli numerycznych ziarna pszenicy odmiany *Eta* oraz wykorzystanie tych modeli do analizy wybranych cech geometrycznych. Do budowy modeli geometrycznych wykorzystano programy komputerowe ScanStudio HD PRO, FreeCAD oraz MeshLab. Za pomocą podstawowych brył geometrycznych oraz dostępnych funkcji rysunkowych w programie FreeCAD zbudowano dziesięć modeli geometrycznych o kształcie zbliżonym do ziarna pszenicy. Porównanie geometrii modeli numerycznych i modeli geometrycznych wykonano programem GOM Inspect. Określano pole powierzchni, objętość oraz dokładne wymiary geometryczne modeli. Wykonano mapy odchyłek wymiarów dla badanych modeli geometrycznych. Błąd względny pomiaru pola powierzchni dla modelu geometrycznego zbudowanego jako bryła obrotowa na podstawie obrysu wykonanego za pomocą łamanej był najmniejszy i wynosił 0,36%. Błąd względny dla kuli wynosił 4,44%. Błąd względny dla modelu geometrycznego zbudowanego jako bryła obrotowa z wykorzystaniem obrysu wykonanego za pomocą dwóch łuków oraz modelu geometrycznego zbudowanego jako bryła obrotowa z wykorzystaniem obrysu wykonanego za pomocą trzech łuków wynosił około 5%. Błąd metody pomiaru objętości jest najmniejszy dla elipsoidy obrotowej oraz elipsoidy i wynosił odpowiednio 3,58% i 4,48%. Zaproponowane modele geometryczne można wykorzystać w pracach badawczych i projektowych.

Słowa kluczowe: skaner 3D, model geometryczny, ziarno pszenicy, bryła obrotowa